# Glassy dynamics in the exchange bias properties of the iron/iron oxide nanogranular system

D. Fiorani,[1] L. Del Bianco,[2] A. M. Testa,[1] and K. N. Trohidou[3]
[1]*Istituto di Struttura della Materia—CNR, 00016 Monterotondo Scalo (Roma), Italy*
[2]*Dipartimento di Fisica, Università di Bologna and CNR-INFM, I-40127 Bologna, Italy*
[3]*Institute of Materials Science, NCSR Demokritos, 15310 Athens, Greece*
(Received 30 January 2006; published 6 March 2006)

We have observed a glassy dynamics of the exchange bias properties in a granular system composed of Fe nanoparticles dispersed in a structurally and magnetically disordered (cluster glasslike) Fe oxide matrix. The exchange field, measured at $T=5$ K, increases with increasing the time $t_w$ spent at $T=50$ K, after applying the cooling field. During $t_w$, the oxide phase evolves towards a lower energy configuration, resulting in a stronger interface exchange coupling with the Fe particle moments. Monte Carlo simulations on core/shell nanoparticles reproduce such aging effect, provided that a shell random anisotropy is assumed.

DOI: 10.1103/PhysRevB.73.092403 PACS number(s): 75.50.Tt, 75.50.Lk, 75.40.Mg, 75.50.Bb

Exchange bias (EB) effect has been the object of great interest during the last 50 years, but, despite the enormous efforts in theory, modeling, and experimental investigations, especially on ferromagnet/antiferromagnet bilayer systems, many questions on the microscopic mechanism of the phenomenon are still open.[1]

New challenging questions are posed by the observation of EB in nanogranular systems, where one of the two phases is structurally disordered and magnetically frustrated, similar to a spin glass (SG).[2,3] When one phase is ferromagnetic (FM) (or ferrimagnetic, FI) and the other one is SG, playing the role of the antiferromagnet (AF) in pinning the FM magnetization so as to minimize the interface exchange interaction energy, peculiar EB properties are expected. The frozen SG state is characterized by a hierarchical organization of metastable states separated by energy barriers of different heights (multivalley energy structure).[4] When the two-phase system is cooled down in a magnetic field ($H_{cool}$) across the glass temperature, a spin configuration of the SG phase will be selected, among the possible ones, through the interface exchange coupling with the FM phase, which in turn favors the FM magnetization to be aligned in the field-cooling direction (unidirectional anisotropy). Thus, depending on the value of the cooling field and on the temperature at which it is applied, the degeneracy of the SG state can be reduced. Hence the magnetothermal history of the sample strongly affects the EB properties, which strictly depend on the interface spin configuration.[5]

A further characteristic of the SG state, as well as of other disordered systems characterized by a collective nonequilibrium dynamics, is the aging effect, i.e., the slowing down of the spin dynamics with increasing the time (waiting time) spent in the frozen state, before any field variation.[6,7] Below the glass temperature, the relaxation rate of the zero-field-cooled magnetization ($M_{ZFC}$) and of the thermoremanent magnetization (TRM) decreases with increasing the time elapsing before the application of the magnetic field and the time of application of the cooling magnetic field before removing it, respectively. The effect reflects the shift, towards longer times, of the spectrum of relaxation times (which are associated to the distribution of energy barriers), due to the evolution of the system towards a lower energy configuration.

In this context, we have investigated the EB properties of a nanogranular system composed of iron particles (mean size $\sim$6 nm) dispersed in a structurally and magnetically disordered iron oxide matrix (a mixture of $Fe_3O_4$ and $\gamma$-$Fe_2O_3$; mean grain size $\sim$2 nm). The technique for the synthesis of the samples, based on a gas-phase condensation method, and the structural characterization tools are described elsewhere.[3] In agreement with previous investigations,[3] the prepared samples show a progressive freezing, with decreasing temperature, of the net moments of interacting oxide regions, resulting in a disordered and frustrated magnetic state, recalling a cluster-glass. The low-field freezing temperature distribution is centered at $T=150$ K. Below $T\sim25$ K, the freezing is complete and the interplay between the different types of interactions (dipolar interparticle, superexchange interoxide, and particle-oxide, which all can be both F and AF in sign) results in a disordered and frustrated frozen state for the whole system.

Below $T=150$ K, a shift of the hysteresis loop towards the negative field values is measured after field-cooling from $T=250$ K, due to the interface exchange coupling between the spins of the Fe particles and the frozen spins of the oxide regions. Due to the disorder of the oxide matrix, multiple random (i.e., with a different mixing of FM and AF interactions) interfaces are likely to be present, as well as different random anisotropies, strong enough to pin the magnetization of the Fe particles. With decreasing the temperature where the loop is measured, the shift strongly increases, also because more and more oxide moments freeze.[5] The value of the loop shift is expressed by the exchange field $H_{ex}=-(H_{right}+H_{left})/2$ and the coercivity is defined as $H_c=(H_{right}-H_{left})/2$, $H_{right}$ and $H_{left}$ being the points where the loop intersects the field axis. Both $H_{ex}$ and $H_c$ were found to strongly depend on $H_{cool}$, going through a maximum (e.g., at $T=5$ K, the maximum values are $H_{ex}\sim500$ Oe and $H_c\sim1670$ Oe for $H_{cool}=4$ kOe).[5]

Here we report an analysis of dynamical effects on the EB properties in the iron/iron oxide nanogranular system, through the control of the aging of the system (variation of

 

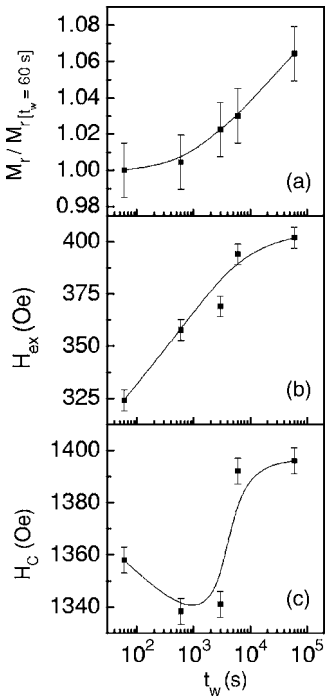


FIG. 1. Remanent magnetization $M_r$ (a), exchange field $H_{\mathrm{ex}}$ (b), and coercivity $H_c$ (c), measured at $T_f=5$ K, as a function of the waiting time $t_w$. $M_r$ is normalized to its value at $t_w=60$ s. Solid line is a guide to the eye.

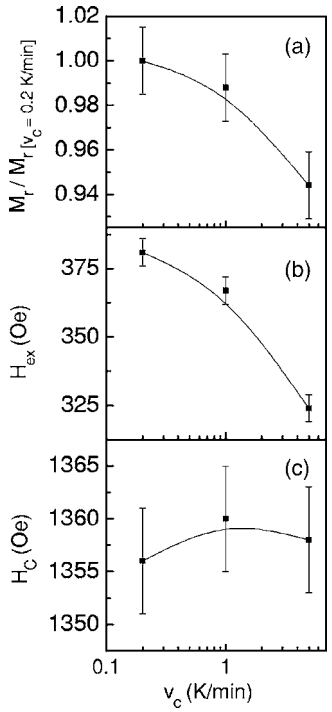


FIG. 2. $M_r$ (a), $H_{\mathrm{ex}}$ (b), and $H_c$ (c), measured at $T_f=5$ K, as a function of the cooling rate $v_c$. $M_r$ is normalized to its value at $v_c=0.2$ K/min.

the waiting time and cooling rate). Moreover, in order to gain a better insight into the origin of such dynamical effects, we have performed Monte Carlo (MC) simulations on isolated, spherical core (FM)/shell (FI) nanoparticles. The MC simulations have shown the capability to predict waiting time effects and to reproduce complicated reversal modes.[8–10]

The effect of the waiting time ($t_w$) was analyzed through the following experiment. The sample was cooled down in zero field from $T=250$ K to $T_i=50$ K. Then, $H_{\mathrm{cool}}=4$ kOe was applied for a time $t_w$ (in the 60–60 000 s range), before starting the field cooling down to $T_f=5$ K (cooling rate $=5$ K/min). At $T_f$, the hysteresis loop was measured, starting from $H=50$ kOe. After each measurement, the sample was warmed up again to $T=250$ K. The evolution of $M_r$, $H_{\mathrm{ex}}$, and $H_c$ with $t_w$ is shown in Fig. 1. $H_{\mathrm{ex}}$ increases monotonously over 20% with increasing $t_w$. A small increase in $M_r$ is also observed. On the other hand, the $H_c$ trend is not regular, but it clearly tends to an increase for the largest values of $t_w$.

Then, we studied the effect of the field-cooling rate. The sample was cooled down (cooling rate=5 K/min) in zero field from 250 K to $T_i=50$ K, where $H_{\mathrm{cool}}=4$ kOe was applied; soon after that, the sample was field cooled at a selected rate $v_c$ (between 5 and 0.2 K/min), down to $T_f=5$ K and the loop was measured. $H_{\mathrm{ex}}$ and $M_r$ increase with decreasing $v_c$ (the change in $H_{\mathrm{ex}}$ is $\sim 18\%$), whereas $H_c$ does not change significantly (Fig. 2).

The aging of the system—namely, the increase in the time spent at a temperature at which most of the oxide moments are frozen, either through an increase of $t_w$ at $T_i$ or through a decrease of $v_c$ from $T_i$ to $T_f$—enhances the EB effect at $T_f=5$ K. In the first experiment, as $t_w$ elapses at $T_i=50$ K, the oxide matrix moments relax towards a more stable energy state, in which the interface exchange interaction energy with the moments of the FM component is minimized. Then, with reducing the temperature from $T_i$ to $T_f$, the system remains trapped in this energy minimum, as it is more difficult to overcome the energy barriers separating different states. It can be easily realized that a similar picture can be drawn for the experiment as a function of $v_c$.

The above description was confirmed by studying the TRM decay. The sample was cooled down in zero field from $T=250$ K to $T_i=50$ K. At $T_i$, $H_{\mathrm{cool}}=4$ kOe was applied for $t_w$, before starting the field cooling down to $T_f=25$ K. At $T_f$, the field was removed and TRM vs time was measured. Both the curves, measured for $t_w=0$ and 6000 s, follow a stretched-exponential decay law, as expected for correlated dynamics in disordered systems,[11] but the relaxation rate is lower for $t_w=6000$ s (Fig. 3). This confirms the slowing down of the dynamics with increasing $t_w$ and hence the $t_w$-dependence of the spin configuration of the relaxing disordered phase. No clear $t_w$-dependence of TRM was observed at $T_f=5$ K. The reason is that, at such a low temperature, the relaxation times are too long for an appreciable relaxation to be observed, at least on the investigated time scale. This was in agreement with previous $M_{\mathrm{ZFC}}$ vs time measurements, showing no relaxation for $T\leqslant 20$ K.[3] Similarly, no change in $H_{\mathrm{ex}}$ was observed after aging the sample directly at $T_f=5$ K, rather than at $T_i=50$ K: at such a low temperature, no appreciable rearrangement in the particle/matrix interface spin configuration occurs, in the investigated time scale. The relaxation process, taking place during $t_w$, results in a net increase of the oxide magnetization along the cooling field direction, accounting for the small increase in

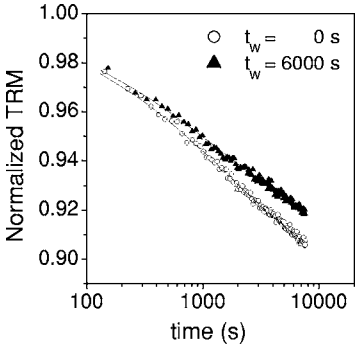


FIG. 3. Thermoremanent magnetization (TRM) vs time, at $T_f = 25$ K, for two different $t_w$ values. TRM is normalized to the value at the beginning of the measurement. The points are fitted by a stretched-exponential decay law (solid lines).

$M_r$ vs $t_w$, at $T_f = 5$ K (Fig. 1), (accordingly, $M_r$ increases with decreasing $v_c$, Fig. 2).

Therefore, by properly aging the sample, a final spin configuration at $T_f = 5$ K is selected, corresponding to a stronger exchange coupling at the particle/matrix interface, which is responsible for the increase in $H_{ex}$ (Figs. 1 and 2).

In the EB phenomenon, a change in $H_{ex}$ is often accompanied by a change in $H_c$.[5,12] In our case, an enhanced $H_c$ is found after waiting for a long $t_w$ (Fig. 1), but fluctuating values are measured at shorter $t_w$ (Fig. 1) and in the case of the measurement as a function of $v_c$ (Fig. 2). The MC simulation, shown just below, confirms this tendency. $H_c$ is scarcely affected by the aging effect, as it also depends on intrinsic sources of anisotropy other than exchange anisotropy.

MC simulations have been carried out to study the $t_w$-dependence of the EB effect in a two-phase magnetic system. We consider spherical nanoparticles of total radii R, expressed in lattice spacings, on a simple cubic (sc) lattice, consisting of a FM core and a FI shell, surrounding the core. The shell thickness is four lattice spacings. The spins in the particles interact with nearest-neighbors Heisenberg exchange interaction, and at each crystal site they experience a uniaxial anisotropy. In the presence of an external magnetic field, the total energy of the system is[13]

$$E = -J_{FM} \sum_{(i,j \in FM)} \vec{S}_i \cdot \vec{S}_j - \sum_{i \in FM} K_{iFM} (\vec{S}_i \cdot \hat{e}_i)^2 - J_{SH} \sum_{(i,j \in SH)} \vec{S}_i \cdot \vec{S}_j - \sum_{i \in SH} K_{iSH} (\vec{S}_i \cdot \hat{e}_i)^2 - J_{IF} \sum_{(i \in FM, j \in SH)} \vec{S}_i \cdot \vec{S}_j - \vec{H} \cdot \sum_i \vec{S}_i .$$

Here $S_i$ is the atomic spin at site $i$ and $\hat{e}_i$ is the unit vector in the direction of the easy axis at site $i$. The first term gives the exchange interaction between the spins in the FM core (exchange coupling constant $J_{FM}$, which is taken equal to one). The second term gives the anisotropy energy of the FM core. If the site $i$ lies in the outer layer of the FM core $K_{iFM} = K_{IF}$ and $K_{iFM} = K_C$ elsewhere. The anisotropy is assumed uniaxial and directed along the z-axis in the whole FM core, including the outer layer facing the FI shell. Due to the reduced symmetry of the interface, the crystal anisotropy at the interface is expected stronger than in the bulk. We take $K_C = 0.05$ and $K_{IF} = 0.5$, one order of magnitude larger than $K_C$. The third term gives the exchange interaction in the FI shell. We set the exchange coupling constant $J_{SH} = -J_{FM}/2$ because the critical temperature of the oxide is lower than the Curie temperature of the corresponding ferromagnet. The fourth term gives the anisotropy energy of the FI shell ($K_{SH} = 1.5$). If the $i$ site lies in the outer layer of the shell then $K_{iSH} = K_S = 1.0$ In this simplified model, the disordered state of the shell is qualitatively reproduced by considering a random anisotropy (at the interface with the FM core, inside the shell, and at the external surface). The fifth term gives the exchange interaction at the interface between the core and the shell. The exchange coupling constant $J_{IF}$ is equal to $J_{SH}$ in size, in agreement with theoretical studies in layered systems[14] and the interaction is considered ferromagnetic. The last term is the energy in the presence of an external magnetic field.

$H$, $H_c$, and $H_{ex}$ are given in units of $J_{FM}/g\mu_B$, T in units $J_{FM}/k$, and the anisotropy coupling constants $K$ in units of $J_{FM}$. $M_r$ is normalized to the magnetization at saturation $M_s$. The cooling field is $h_L = 0.4$, in our units. We simulate the field-cooling procedure starting with the nanoparticle at temperature $T = 3.0$ (for the sc lattice the Curie temperature $T_C = 2.9$). The nanoparticle is cooled down to the temperature of 0.75 in zero field. At $T_i = 0.75$, we apply $h_L$ along the z-axis for different times $t_w$, expressed in Monte Carlo steps (MCS). Then, we continue the field cooling at a constant rate, down to $T_f = 0.01$, where the loop is measured. The MC simulations have been performed using the Metropolis algorithm. It should be noted that the time evolution of the system does not come from any deterministic equation for the magnetization. The obtained dynamics is intrinsic to the MC method.[8,15] This means that our time unit is not related to a real time interval. Thus comparing the measured and simulated data is similar to comparing measurements with different time scales, for example, dc magnetometry and Mössbauer spectroscopy. The results of our MC simulations reproduce qualitatively the trend of the experimental data.

In our simulations, we use $10^4 - 25 \times 10^5$ MCS depending on T and $t_w$. The results were averaged over 100 different *samples* (namely, independent random number sequences corresponding to different realizations of thermal fluctuations) cooled down under the same conditions ($t_w$ and $T_i$). $M_r$, $H_{ex}$, and $H_c$ vs $t_w$ for a particle of radius $R = 9$ are shown in Fig. 4. The three parameters increase with increasing $t_w$, satisfactorily reproducing the qualitative features of the measurements in Fig. 1. It is worth noticing that the MC simulations also reproduce the experimental TRM decay (Fig. 3). In Fig. 5, TMR vs time (in MCS) is plotted for two different $t_w$ values, at the temperature $T_f = 0.15$. The decay is slower at higher $t_w$. Almost no $t_w$-dependence was observed at lower temperature ($T_f = 0.01$).

Finally, we have repeated the calculations considering for the shell a uniaxial anisotropy directed along the z-axis (except for the external surface, where the anisotropy was assumed to be random). No variation of $M_r$, $H_{ex}$, and $H_c$ with $t_w$ was observed, revealing that random anisotropy in the

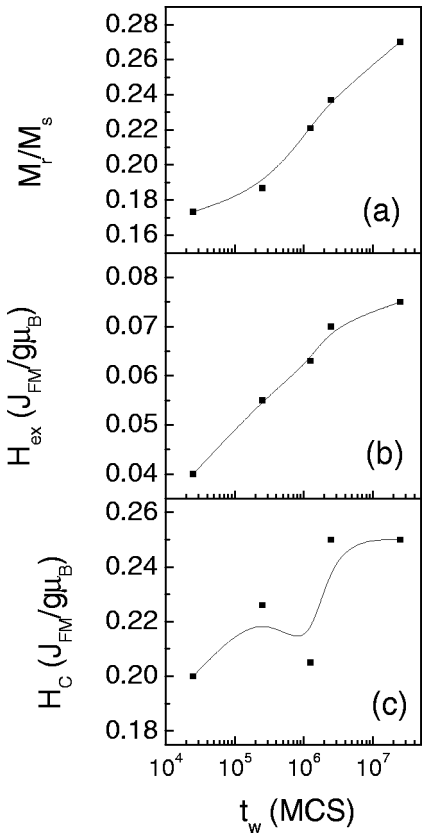


FIG. 4. $M_r$ (a), $H_{ex}$ (b), and $H_c$ (c) vs $t_w$, as obtained by the MC simulations.

shell and at the interface with the FM core is a fundamental ingredient for the appearance of the aging effect.

In conclusion, our results show that dynamical effects have a sizeable influence on the EB properties of the nanogranular iron/iron oxide system. The value of $H_{ex}$ can be controlled by varying $t_w$ at $T_i$ or $v_c$ from $T_i$ to $T_f$. In fact, in this way, one can select the final spin configuration of the disordered oxide phase at the interface with the ordered Fe component. As a consequence, $M_r$ and $H_c$ are also modified. Indeed, the inherent magnetic disorder of the oxide phase is the key factor, allowing $H_{ex}$ to be varied simply through the aging of the sample. This is confirmed by MC simulation results on core(FM)/shell(FI) nanoparticles showing that a glassy dynamics of the EB properties is observed provided that a shell random anisotropy is assumed. The possibility of controlling $H_{ex}$ opens perspectives for technological application in tuning the performance of EB-based magnetic devices.

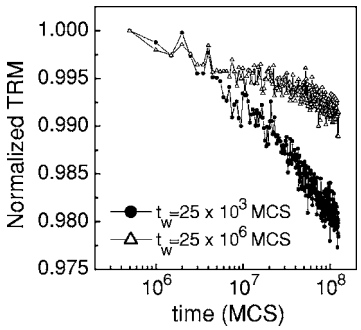


FIG. 5. TRM vs time at $T_f=0.15$ for two different $t_w$ values, as obtained by the MC simulations. TRM is normalized to the value at the beginning of the simulation.

The research was sponsored by MIUR under project FIRB-Magnetic Microsystems. One of the authors (K.N.T.) acknowledges the support of the EU under NANOSPIN Contract No. NMP4-CT-2004-013545.

[1] J. Nogues and I. K. Schuller, J. Magn. Magn. Mater. **192**, 203 (1999).
[2] R. H. Kodama, A. E. Berkowitz, E. J. McNiff, and S. Foner, Phys. Rev. Lett. **77**, 394 (1996).
[3] L. Del Bianco, D. Fiorani, A. M. Testa, E. Bonetti, L. Savini, and S. Signoretti, Phys. Rev. B **66**, 174418 (2002).
[4] K. Binder and A. P. Young, Rev. Mod. Phys. **58**, 801 (1986).
[5] L. Del Bianco, D. Fiorani, A. M. Testa, E. Bonetti, and L. Signorini, Phys. Rev. B **70**, 052401 (2004); L. Del Bianco, D. Fiorani, A. M. Testa, and E. Bonetti, J. Magn. Magn. Mater. **290–291**, 102 (2005).
[6] Ph. Refregier, E. Vincent, J. Hammann, and M. Ocio, J. Phys. (Paris) **48**, 1533 (1987).
[7] T. Jonsson, J. Mattsson, C. Djurberg, F. A. Khan, P. Nordblad, and P. Svedlindh, Phys. Rev. Lett. **75**, 4138 (1995).
[8] K. Binder, *Monte Carlo Methods in Statistical Physics* (Springer, Berlin, 1979).
[9] A. Lyberatos, J. Earl, and R. W. Chantrell, Phys. Rev. B **53**, 5493 (1996); G. Suran, J. J. Arnaudas, M. Ciria, C. Fuente, M. Rivoire, O. A. Chubykalo, and J. M. Gonzalez, Europhys. Lett. **41**, 671 (1998).
[10] J. H. Toloza, F. A. Tamarit, and S. A. Cannas, Phys. Rev. B **58**, R8885 (1998); J.-O. Andersson and P. Svedlindh, J. Magn. Magn. Mater. **104–107**, 1609 (1992).
[11] R. V. Chamberlin, G. Mozurkewich, and R. Orbach, Phys. Rev. Lett. **52**, 867 (1984).
[12] T. Ambrose, R. L. Sommer, and C. L. Chien, Phys. Rev. B **56**, 83 (1997); D. V. Dimitrov, S. Zhang, J. Q. Xiao, G. C. Hadjipanayis, and C. Prados, *ibid.* **58**, 12090 (1998).
[13] E. Eftaxias and K. N. Trohidou, Phys. Rev. B **71**, 134406 (2005).
[14] T. C. Schulthess and W. H. Butler, Phys. Rev. Lett. **81**, 4516 (1998); U. Nowak, K. D. Usadel, J. Keller, P. Miltenyi, B. Beschoten, and G. Guntherodt, Phys. Rev. B **66**, 014430 (2002).
[15] L. C. Sampaio, M. P. de Albuquerque, and F. S. de Menezes, Phys. Rev. B **54**, 6465 (1996); J. M. Gonzalez, O. A. Chubykalo, and R. Smirnov-Rueda, J. Magn. Magn. Mater. **203**, 18 (1999).